The dynamics of spawning acts by a semelparous fish and its associated energetic expenses

Cédric TENTELIER[1,2,a], Colin BOUCHARD[1,2,3,b], Anaïs BERNARDIN[1], Amandine TAUZIN[1], Jean-Christophe AYMES[1,2,c], Frédéric LANGE[1,2,d], Charlotte RECAPET[1,2,e], Jacques RIVES[1,2,f]

[1] Universite de Pau et des Pays de l'Adour, E2S UPPA, INRAE, ECOBIOP, Saint-Pée-sur-Nivelle, France

[2] Pôle Gestion des Migrateurs Amphihalins dans leur Environnement, OFB, INRAE, AGROCAMPUS OUEST, UNIV PAU & PAYS ADOUR/E2S UPPA

[3] Tour du Valat, Research Institute for the Conservation of Mediterranean Wetlands, Arles, France

[a] ORCID: 0000-0003-2178-4900
[b] ORCID: 0000-0003-0845-9492
[c] ORCID: 0000-0002-1181-3010
[d] ORCID: 0000-0001-8561-1879
[e] ORCID: 0000-0001-5414-8412
[f] ORCID: 0000-0001-6074-3488

Corresponding author: Cédric TENTELIER,

Univ. Pau & Pays Adour

Collège STEE – Campus de la côte basque

1 allée du parc Montaury

64 600 Anglet, France.

cedric.tentelier@univ-pau.fr

Abstract

1. During the reproductive season, animals have to manage both their energetic and gametic budgets. In particular, for semelparous capital breeders with determinate fecundity and no parental care other than gametic investment, the depletion of energetic stock must match the depletion of gametic stock, so that individuals get exhausted just after their last egg is laid. Although these budgets are managed continuously, monitoring the dynamics of mating acts and energy expenditure at a fine temporal scale in the wild is challenging.

2. This study aimed to quantify the individual dynamics of spawning acts and the concomitant energy expenditure of female Allis shad (*Alosa alosa*) throughout their mating season.

3. Using eight individual-borne accelerometers for one month, we collected tri-axial acceleration, temperature, and pressure data that we analysed to i) detect the timing of spawning acts, ii) estimate energy expenditure from tail beat frequency and water temperature, and iii) monitor changes in body roundness from the position of the dorsally-mounted tag relative to the vertical.

4. Female shad had a higher probability to spawn during warmer nights, and their spawning acts were synchronized within each active night. They underwent warmer temperature during the day, when they stayed deeper, and they swam faster at night, when they spent more energy. Over one month of spawning, they performed on average 15.75 spawning acts, spent on average 6 277 kJ and died with a significant portion of residual oocytes. The acceleration-based indicator of body roundness was correlated to condition coefficient measured at capture, and globally decreased through the spawning season, although the indicator was noisy and was not correlated to changes in estimated energy expenditure.

5. Despite significant individual variability, our results indicate that female shad exhausted their energetic stock faster than their egg stock. Water warming might accentuate the mismatch

54 between energetic and gametic stocks. Although perfectible, the three complimentary analyses
55 of acceleration data are promising for *in situ* monitoring of energy expenditure related to
56 specific behaviour.

57 ## Keywords

58 Accelerometer, biologging, clupeid, egg retention, energy budget, reproductive effort,
59 semelparity, temperature, thinning.

60

Introduction

The energy acquired by living organisms is allocated to survival and reproduction, and natural selection is expected to favour optimal allocation, resulting in life-histories that maximize Darwinian fitness in the environment where evolution occurs (Pianka 1976; Stearns 1992; Roff 1993). When adult survival is low compared to juvenile survival, extreme reproductive effort (in gametogenesis, mating behaviour and parental care) can be selected and semelparity may arise, in which individuals die after their first and only breeding season. Semelparity is often accompanied with capital breeding, so that reproduction relies on energy reserves constituted before the breeding season (Bonnet et al. 1998). Although semelparity is sometimes quoted as “big bang reproduction”, its broad definition encompasses cases where individuals breed in several bouts within a breeding season (Kirkendall and Stenseth 1985; Hughes 2017). Furthermore, in species with no other parental care than gametic investment, the optimal allocation should result in individuals dying just after their last progeny is produced, and deviation from optimality consists in individuals either surviving after their last egg is laid, or dying of exhaustion while still bearing unlaid eggs (Heimpel and Rosenheim 1998). Hence, the schedule of breeding events and the dynamics of energy expenditure during the breeding season, which may be steep in semelparous capital breeders, is a crucial aspect of reproductive strategy. Beside energy expenditure, the temporal distribution of breeding events within a season may be linked to social factors that synchronize breeding and affect the mating system of the population (Emlen and Oring 1977).

Tracking the schedule of breeding events and the dynamics of energy expenditure of breeding individuals in the wild is technically challenging. The timing of breeding events along the breeding season requires thorough observation of repeatedly detectable individuals, for example through video supervision of highly sedentary individuals (e.g. Borgia 1985). Energy expenditure has been monitored at the population level, by quantifying energy reserves on

different individuals sampled at different stages of the breeding season (e.g. Hendry and Berg 1999). In some cases, the same individuals were captured at the beginning and at the end of the breeding season, and the energy expenditure quantified with difference in weight (Anderson and Fedak 1985; Rands et al. 2006), body composition (Hendry and Beall 2004; Casas et al. 2005), or concentration of plasma metabolites (Gauthey et al. 2015). Likewise, in terrestrial animals, the turnover of ^{18}O and ^{2}H from doubly labelled water quantifies the average field metabolic rate at the individual level between two sampling occasions (Nagy et al. 1999). All these methods give a good idea of the total energy expenditure over the whole breeding season but often lack the temporal resolution to document the longitudinal dynamics of energy expenditure all along the breeding season.

With the advent of bio-logging, the temporal resolution of individual data collected in the field has tremendously increased. Among bio-loggers, accelerometers, often coupled with other sensors such as thermometers, have been increasingly used, and advances in their energetic efficiency now allows to record high-frequency data for weeks or months, making them valuable tools for longitudinal studies of breeding behaviour in many organisms. In this context, acceleration data can quantify both the overall movement of tagged individuals, which can be translated in energy through laboratory calibration (Wilson et al. 2006; Groscolas et al. 2010; Collins et al. 2016; Hicks et al. 2017), and the number and temporal distribution of key behaviours such as mating events, if these produce a typical acceleration pattern (Brown et al. 2013).

This study aimed at describing the activity and change in body condition of female semelparous fish throughout their spawning season. Using accelerometers, we investigated three main aspects:

1) The schedule of spawning events was identified using a characteristic acceleration. We tested whether the timing of spawning events was influenced by temperature and whether it was synchronized within and among females.
2) The global activity was quantified as tail beat frequency, and converted to energy expenditure through an energetic model including water temperature. This was used to identify variability in energy expenditure between individuals and between periods of the spawning season.
3) We tested the possibility to use the angle between the dorsally-mounted accelerometer and the vertical as an indicator of body roundness of the fish. This would allow monitoring the thinning process through the spawning season, and relate it to periods of high energy expenditure.

Egg load at the death of individuals was also measured to test the relationship between spawning dynamics, energy expenditure and quantity of unspent eggs.

Methods

Characteristics of the species studied, and predictions

Allis shad (*Alosa alosa* L.) is an anadromous clupeid fish distributed along the Atlantic coast of Europe, from Portugal to the British Isles, with the main populations dwelling in the French rivers Garonne, Dordogne and Loire (Baglinière and Elie 2000). Across its distribution, Allis shad is considered as a semelparous species, although spawning marks on scales suggest that a very small proportion of individuals may spawn on two consecutive years (Mennesson-Boisneau and Boisneau 1990; Taverny 1991). After having spent a few months in freshwater as juveniles and four to six years at sea, shad undertake freshwater upstream migration during which they fast, thus qualifying as capital breeders. Gonad maturation occurring during

133 migration leads females to bear between 13 000 and 576 000 eggs, reaching an average gonad
134 mass of 221 g and a gonad / somatic weight ratio of 15% on spawning grounds (Cassou-Leins
135 and Cassou-Leins 1981; Taverny 1991). Spawning typically occurs at night in a 0.3 to 3 metre-
136 deep glide. The spawning act consists of at least one male and one female swimming side by
137 side during five to ten seconds while describing three to five circles of one meter in diameter
138 and beating the water surface vigorously with their tail (Baglinière and Elie 2000). The typical
139 splashing noise (35 dB at one meter) can be heard and recorded from the river bank, and the
140 number of splashes recorded during the spawning season is often used as an indicator of the
141 number of spawners in a population (Chanseau et al. 2004).

142 Although very few data are available, the number of splashes recorded upstream from
143 dams where migrating shad were counted suggest that females perform on average five to
144 twelve spawning acts during the season (Fatin and Dartiguelongue 1996; Acolas et al. 2006
145 Apr). Moreover, based on the dynamics of ovary index and oocyte diameter measured on
146 individual caught and dissected across the season, Cassou-Leins & Cassou-Leins (1981)
147 postulated that shad mature their eggs in five to seven batches. We therefore expected the
148 number of spawning acts recorded by the individual-borne accelerometers to be between five
149 and twelve, separated with a regular delay corresponding to the maturation time of each egg
150 batch.

151 The spawning season spans from early-May to late July, but dead individuals can be
152 collected downstream from spawning ground as soon as late May, so we expected individual
153 reproductive lifespan to be around one month. The number of splashes heard on spawning
154 ground increases with increasing water temperature (Baglinière and Elie 2000; Paumier et al.
155 2019). This could be due to either more individuals being sexually active or individuals to be
156 more active at higher temperature. Hence, we expect a positive effect of water temperature
157 during a night on either the individual probability of performing at least one mating act during

158 that night or the number of mating acts performed by each individual active on that night.
159 Within a night, the temporal distribution of splashes typically follows a Gaussian distribution
160 centred on 2 AM and spanning from 10 PM to 6 AM (Cassou-Leins and Cassou-Leins 1981).
161 However, this was observed mainly for large populations with thousands of spawners and
162 hundreds of splashes per night. In the case of a small population, the temporal distribution may
163 depart from this particular Gaussian distribution. In particular, the aggregative behaviour of
164 shad, which shoal even during the spawning season (Baglinière and Elie 2000), suggests that
165 females may synchronize their spawning acts within a night.

166 Shad being capital breeders, samples of different individuals caught at different times
167 during the migration have shown dramatic changes in somatic mass and tissue composition
168 (Cassou-Leins and Cassou-Leins 1981; Bengen 1992), but no longitudinal data exist at the
169 individual level. We expected that shad would get thinner as the season progresses, and all the
170 more so during periods of high energy expenditure due to warm water (recorded by individual-
171 borne thermometers) or intense activity (recorded by individual-borne accelerometers). If the
172 angle of the accelerometer with the vertical is a good indicator of the individual's roundness, it
173 should be correlated to individual coefficient of condition when fish are measured and weighed.
174 It should also decrease throughout the spawning season as the fish thins, and its shift during a
175 period of the season should be correlated to the energy expenditure during this period.

176 Because shad are nocturnal and capital breeders, they were expected to rest during the
177 day in order to save energy and survive until they have laid all their eggs. We therefore predicted
178 that shad should swim slowly and stay in deeper, cooler water during the day, and be more
179 active and in shallow water during the night (Baglinière and Elie 2000). Accordingly, their
180 energy expenditure should be lower during the day than during the night, and their body
181 condition was expected to decrease faster during the night than during the day. Finally, facing
182 the risk of death before having laid all eggs, shad which have well managed their energy were

183 expected to die with less residual eggs. We therefore predicted that the mass of residual eggs at
184 death should be linked negatively with the number of spawning acts and energy expenditure
185 during the night, and positively with energy expenditure during the day.
186

187 ## Fieldwork

188 We conducted this study in spring 2017 and 2018 in the Nivelle, a 39 km long coastal
189 river situated in the Northern Basque Country, France, and draining a 238 km² basin. The
190 downstream limit of the study zone was the impassable Uxondoa weir, situated 12 km upstream
191 from the river mouth (43°21'40.64"N, 1°35'13.99"W), and equipped with a vertical slot fishway
192 and a trap where a yearly average of 230 (min = 26; max = 688) migrating shad have been
193 counted since 1996, with less than 30 individuals per year since 2015. Five kilometres upstream
194 from Uxondoa stands another impassable weir equipped with a fishway and a trap, where shad
195 have almost never been captured.
196 The Uxondoa fish trap was controlled daily throughout spring (ECP 2018). Nine female
197 shad were captured and tagged in 2017, and 15 in 2018. All experimental procedures comply
198 with French and European legislation, and were approved by the legal representative
199 (prefectural decree #64-2017-04-25-004) and the ethical committee for birds and fishes in the
200 French region Nouvelle Aquitaine (authorization #2016020116037869). The tagging procedure
201 was quite similar to Breine (2017) for twaite shad (*Alosa fallax*). We anesthetized each
202 individual in a bath of 15 mg/L benzocaine diluted in river water before to weigh it, measure
203 its fork length, and finally tag it with a radio transmitter emitting at a unique frequency (F2020,
204 ATS, Isanti, MN, USA) and a three-dimensional accelerometer (WACU, Atesys-Montoux,
205 Huguenau, France). For tagging, each fish was kept in a 20 L tank filled with anaesthetic
206 solution. A water pump placed in the fish's mouth and a stone bubbler in the bath ensured a
207 good circulation of aerated water during the tagging procedure. Adjustable plastic plates

208 covered with foam were placed vertically against both flanks to maintain the fish in an upright
209 position, with only its back being above water surface. The radio transmitter and the
210 accelerometer were cleaned with a povidone iodine solution (Betadine®) and dried with
211 surgical cotton. The two Teflon-coated metallic wires of the radio transmitter were inserted
212 approximately 1 cm under the dorsal fin through sterile hollow needles. The hollow needles
213 were then removed, and the metallic wires were passed through holes drilled in the
214 accelerometer's lug, secured with plastic eyelets and aluminium sleeves, and the extra length
215 was cut. The radio transmitter and the accelerometer weighed 8.6 g and 9 g, respectively, so the
216 weight was balanced on both sides of the fish. After tagging, each fish was placed in a 50 L box
217 filled with river water, and released upstream from the weir upon waking.

218 From its release at Uxondoa weir until its death at the end of the spawning season, each
219 tagged shad was localized twice a day using a mobile receiver (R2100, ATS, Isanti, MN, USA)
220 and a loop antenna, in order to check whether it was still alive and to obtain its position. The
221 radio transmitters were set to double their pulsing rate after 8 h of total immobility. Within two
222 days after double pulse was detected, the dead fish and the tags were recovered by snorkelling,
223 and the whole fish and its ovaries were immediately weighed.

224

225 ## Processing acceleration data

226 The loggers used in this study recorded acceleration between -8 g and +8 g (1 g = 9.81
227 $m.s^{-2}$) in each of the three dimensions at an average frequency of 50 logs per second. Every
228 second, they also recorded the temperature, pressure, date, time and exact number of
229 acceleration logs within the past second. Both dynamic and static (gravitational) acceleration
230 were used to estimate three types of variables: body roundness through the angle of the
231 accelerometer with the vertical, tail beat frequency and occurrence of spawning acts.

The static, gravitational, component on each axis i (x, y and z) was extracted from the raw signal at each time t by replacing each data point $\overrightarrow{A_{i,t}}$ by the average of the points within a window of width w centred on t, so that:

$$\overrightarrow{SA_{i,t}} = \frac{1}{w}\sum_{j=t-\frac{w}{2}}^{j=t+\frac{w}{2}} \overrightarrow{A_{i,J}}$$

Unlike what is usually done (Brown et al. 2013), these data were not used to assess the posture of the fish, as no known behaviour in shad involves change of posture. Instead, we hypothesized that it may reflect the shape of the fish. Indeed, since the accelerometer was pinned on the dorsal part of the fish's flank, the angle θ between the x-axis of the tag and the vertical may be linked to the roundness of the fish, a proxy of its energetic reserves. This angle could be computed at any data point of static acceleration, as $\theta_t = cos^{-1}(\overrightarrow{SA_{x,t}})$, where θ_t is the angle at time t and $\overrightarrow{SA_{x,t}}$ is the static acceleration computed on the x-axis at time t (Fig. 1.A). To track change in body roundness through the season, θ was estimated for each fish from $\overrightarrow{SA_{x,t}}$ computed over w=180 000 points (*i.e.* 1 h at a 50Hz sampling frequency) every eight hours (6AM, 2PM, 10PM), from its release until its death.

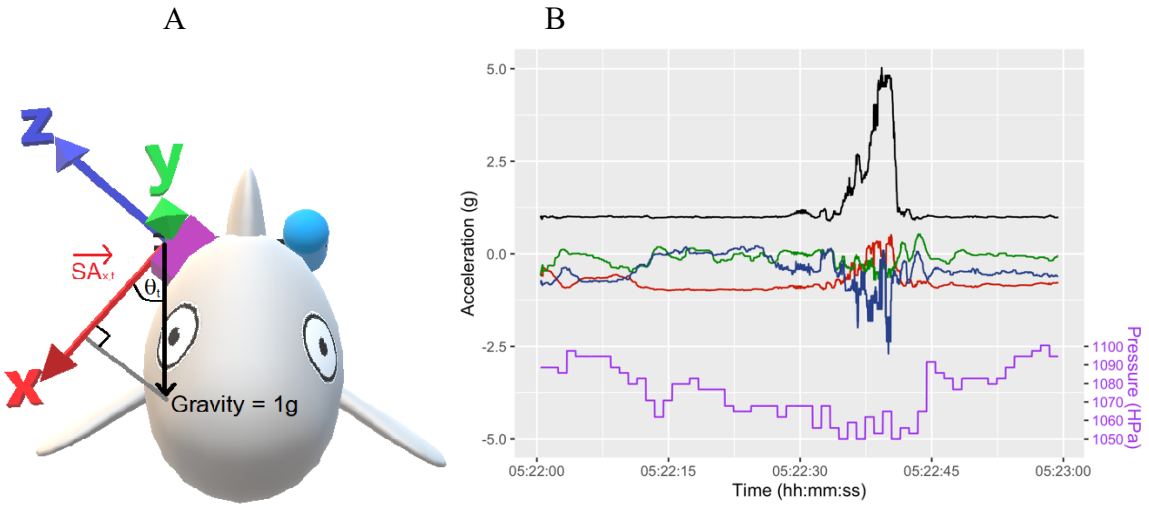

Figure 1. Allis shad were tagged with a radio transmitter on the left flank and an accelerometer on the right flank. The accelerometer continuously recorded acceleration on three axes. A. The static component of acceleration recorded on the x-axis at time *t*, $\overrightarrow{SA_{x,t}}$, corresponds to the orthogonal projection of gravity, which is vertical by definition, on this axis. Hence, the angle θ between the x-axis and the vertical can be computed for any time *t* as $\theta_t = cos^{-1}(\overrightarrow{SA_{x,t}})$. B. The dynamic component of acceleration (smoothed with a 250-point wide median filter) can be used to detect spawning acts, characterized by increased acceleration on both x (red), y (green) and y (blue) axes, resulting in a peak in the norm of the 3-dimensional acceleration vector (black), and accompanied by a decrease in hydrostatic pressure (purple).

The dynamic component of acceleration was computed at every time point on each dimension *i* ($\overrightarrow{DA_{i,t}}$) as the raw signal minus the static acceleration computed over *w*=250 points (=5 s at 50 Hz). This was used to quantify the activity of the fish through Tail Beat Frequency (TBF), computed as the number of zero-crossings of $\overrightarrow{RDA_{z,t}}$ per second. TBF can be computed at every instant, but for further analysis we used average computed for every minute.

We estimated the energy consumption for every minute of each individual's reproductive season, using its tail beat frequency (computed as described above), the temperature recorded by the individual logger, and equations derived from the data of Leonard et al. (1999) and Castro-Santos & Letcher (2010) on American shad, *Alosa sapidissima*. Leonard et al. (1999) measured oxygen consumption and tail beat frequency of 18 American shad in a swimming respirometer with water temperature varying between 13°C and 24°C. On their data, we fitted a linear mixed model (lmer function in lme4 package; Bates et al. 2014) with individual random intercept and fixed effects of temperature and TBF, on log-transformed oxygen demand (MO_2, in mmol $O_2.kg^{-1}.h^{-1}$). Then, assuming that 0.4352 kJ of somatic energy are burnt per mmol O_2 (Brett and Groves 1979), we used the three parameters of the mixed

model (average intercept = 1.0064, slope of temperature = 0.0531, and slope of TBF = 0.2380) to compute the amount of energy $E_{i,t}$ (in kJ) consumed by each fish i for each minute t of its spawning period, from its body mass $M_{i,t}$ (in kg), the average temperature recorded by its logger during that minute $T_{i,t}$ (in °C), and its average tail beat frequency during that minute $TBF_{i,t}$ (in beat per second):

$$E_{i,t} = \frac{1}{60} \times 0.4352 \times M_{i,t} \times e^{1.0064+0.0531\times T_{i,t}+0.2380\times TBF_{i,t}} \quad \text{(Equation 1)}$$

Since energy consumption continually reduces fish mass, we iteratively modelled fish mass and energy expenditure at each minute of the spawning season. For this, we assumed that shad get 69% of their energy from lipids and 31% from proteins to fuel their metabolism (Leonard & McCormick, 1999), and that one gram of fat yields 39.54 kJ, against 23.64 kJ per gram of protein (Craig et al. 1978), so fish mass at the t^{th} minute was:

$$M_{i,t} = M_{i,t-1} - \frac{E_{i,t}}{0.69\times 39.54+0.31\times 23.64}.10^{-3} \quad \text{(Equation 2)}$$

The dynamic acceleration was also used to count the number of spawning events performed by each tagged shad. To do this, the acceleration pattern typical of spawning act was first described in a controlled experiment and then searched in the field-collected data. To characterize the typical pattern associated with spawning act, a male and a female shad were captured at Uxondoa trap, tagged as described above, and observed for one month (June 2016) in a basin (400 m², 0.6 m water depth) at the INRAE experimental facilities in St Pée sur Nivelle (ECP 2018). Eight spawning acts were recorded on video or audio, which could be paralleled with acceleration data. The typical pattern of acceleration associated to the spawning act was a rise in the norm of the 3D acceleration vector, which stayed above 3 g for at least 3 seconds, mainly driven by acceleration on the z-axis corresponding to TBF reaching up to 15 beats per second. A decrease of hydrostatic pressure was typically associated to this pattern, due to the fish reaching the water surface during the spawning act (Fig. 1.B). These criteria for identification of spawning acts were robust, as they were always detected when spawning was

visually observed (no false negative) and never observed when spawning was not visually observed (no false positive). These criteria were implemented in an algorithm to scan the accelerograms collected in the field in 2017. This automated identification was validated by visual comparison of accelerogram sequences automatically identified in 2017 with sequences of eight acknowledged spawning acts recorded in 2016.

Finally, the exact timing of each individual's death was detected as a clear change in the acceleration signal, where the gravitational component indicated that the fish switched from upright posture to lying on its side or upside down, and the only dynamic component left was the tenuous jiggling due to water flowing over the tag.

Statistical analysis

All analyses were performed on R (R Development Core Team 2008). A zero-inflated mixed regression (package glmmTMB; Brooks et al. 2017) was used to test the effect of temperature on the number of spawning acts performed by each individual on each night. The Binomial component of the model informed on the effect of temperature on the probability to perform any spawning act, while the Poisson component tested the effect of temperature on the number of spawning acts. Individual was used as a random effect on both components. At a finer timescale, we tested whether females spawning in the same night synchronized their spawning acts. To do this, we performed 10 000 permutations of the hour of spawning acts recorded along all nights, and compared the median of the delay to the nearest spawning act for actual data and for simulated data. Because our aim was not to test the synchrony between acts performed by the same female, only the first act performed by each female on a given night was considered in this analysis.

As mentioned above, TBF was computed for every minute of each individual's spawning season, to track its energy expenditure. As an indicator of fish activity, average TBF

was also aggregated over eight-hour time windows corresponding to three periods of the day: morning (6AM-2PM), afternoon (2PM-10PM) and night (10PM-6AM). The limits of the night period correspond to the earliest and latest hour of spawning activity classically recorded on spawning grounds (Cassou-Leins and Cassou-Leins 1981). To test whether shad adopted a different behaviour at different periods of the day, linear mixed models with individual random intercept and period of the day as a fixed effect were fitted to TBF, temperature and depth. For TBF, we also added a binary covariate indicating whether the fish had been tagged for more or less than three days, to test whether recent tagging impaired activity (Føre et al. 2020 Apr 21). Depth was estimated by computing hydrostatic pressure ($1 hPa.cm^{-1}$) as the difference of pressure recorded every second by each tag and the atmospheric pressure recorded every 20 minutes by a meteorological station situated at the INRAE facilities, less than one kilometre from the spawning ground. All mixed models were fitted using the package lme4 for R (Bates et al. 2014), significance of fixed effects was tested using the likelihood ratio test (LRT χ^2) between the model including the fixed effect and the nested model excluding it. Marginal and conditional R^2 (R^2_m and R^2_c), indicating the proportion of variance explained by the fixed effects and by the whole model, respectively, where computed using R package MuMIn (Barton 2009).

To our knowledge, static acceleration has never been used to assess changes in animal body roundness. We tested three predictions resulting from the hypothesis that the angle θ between the x-axis of an individual's accelerometer and the vertical was an indicator of body roundness. First, we fitted a Pearson correlation between Fulton condition coefficient (100*weight (in grams)/length (in centimetres)^3) and θ, both measured at the initial capture and at death. Second, a linear mixed model, with individual random intercept and slope was used to test whether θ decreased with time since individual release. Third, to test if change in θ over the breeding season was proportional to change in condition, a correlation was performed between the differences in θ and in Fulton condition coefficient from release to death. Finally,

to test whether the decrease in θ could be linked to temperature, activity, energy expenditure or the moment of the days, we fitted linear mixed models with the difference in θ between the first and the last hour of each 8-hour period and an individual random intercept. Four models were tested, 1) the null model with only random intercept, 2) a model with average temperature and TBF during the 8-hour period as fixed effects, 3) a model with cumulated energy expenditure during the 8-hour period as a fixed effect, and 4) a model with the moment of the period (morning, afternoon, night) as a fixed effect. To compare mixed models corresponding to alternative hypotheses, we used Akaike Information Criterion corrected for small sample bias (AICc) on R package MuMIn (Barton 2009).

The R code for statistical analysis and the data sets on which they were performed are available in the institutional data repository of the INRAE (French National Institute for Agriculture Food and Environment): https://doi.org/10.15454/NTFYCC.

Results

The nine female shad tagged in 2017 survived between 20 and 37 days (mean=26 days), and all tags were retrieved within one or two days after fish died, although one tag stopped recording data after ten days. The 2018 campaign was much less successful: two fish died one week after tagging, before any spawning acts were recorded; two fish lost their tags three and four days after tagging. The eleven remaining fish were radio tracked throughout the spawning season, until two exceptional floods (on June 7th and 16th) flushed them down to the estuary and the ocean where high water conductivity prevented further radio tracking, hence tag retrieval. Eventually, among the 25 tagged shad, only eight fully exploitable and one partially exploitable accelerograms could be collected. This sample of eight females represented half of the females

that passed the Uxondoa weir in 2017, but the power of Spearman correlations to detect even a strong correlation of 0.5 between variables observed at the individual level was only 0.22.

According to their accelerograms, the eight female shad performed 7, 9, 12, 14, 14, 17, 24 and 26 spawning acts (mean=15.75). The total number of spawning acts performed by each female was correlated to none of the individual variables tested (Fig. 2).

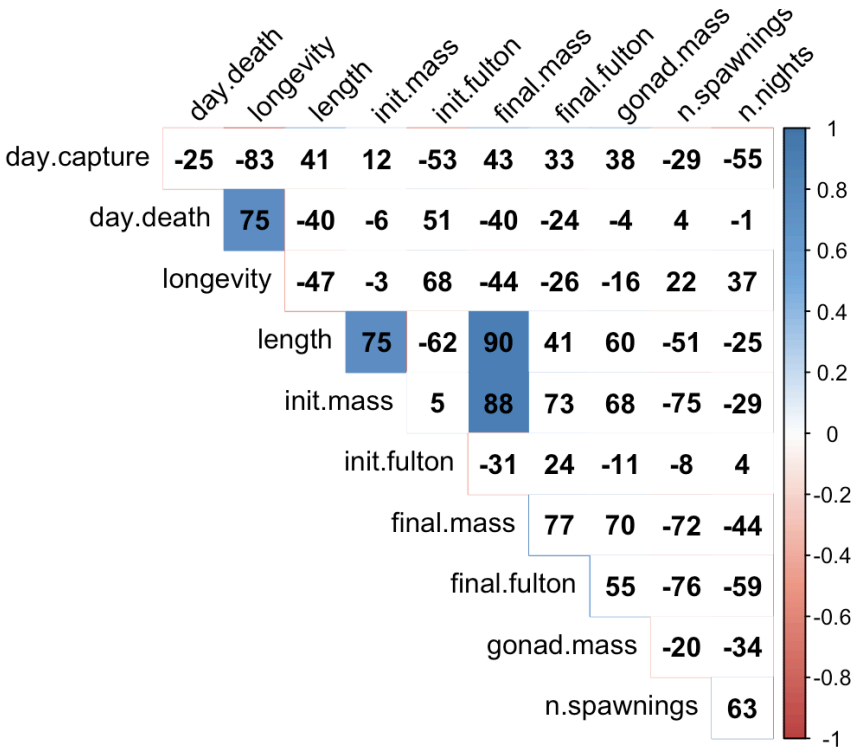

Figure 2. Spearman coefficient of correlation (expressed as percentage) between biometric and reproductive variables of female Allis shad. In order, day of capture, day of death, number of days between capture and death, body length, initial mass, initial Fulton coefficient of condition, final mass, final Fulton coefficient of condition, final gonad mass, number of spawning acts, number of nights with at least one spawning act.

For each female, spawning acts were distributed in three to six nights (mean=4.87) each separated by zero to eight nights (mean=3.55) without spawning acts, resulting in individual spawning seasons ranging from 14 to 24 nights (mean=18.12) from the first spawning act to the

last (Fig. 3.A). The tagged females performed their first spawning act zero to eight days after tagging (mean=3). Only on eight occasions did a female perform a single spawning act during a night, so the 137 remaining acts were performed in volleys. At the individual level, an active night comprised from two to eight acts (mean=3.23) performed in two to 84 minutes (mean=29.7). The mixed zero-inflated Poisson regression indicated that water temperature during the night had a positive effect on the probability that a female performed at least one spawning act (negative effect on the zero inflation; z=-1.95, p=0.05) but no effect on the number of spawning acts in the volley (the Poisson component; z=-1.44, p=0.15). Cumulated over all the season, the temporal distribution of spawning acts within the night followed a Normal distribution, centred on 3AM, with 95% of spawning acts occurring between 0:30AM and 5:30AM. However, the permutation test on the hour of spawning acts indicated synchrony between acts performed by different females on the same night: the median time lag to the nearest act was one hour for observed data, which corresponds to the first percentile of simulated data (Fig. 3.B).

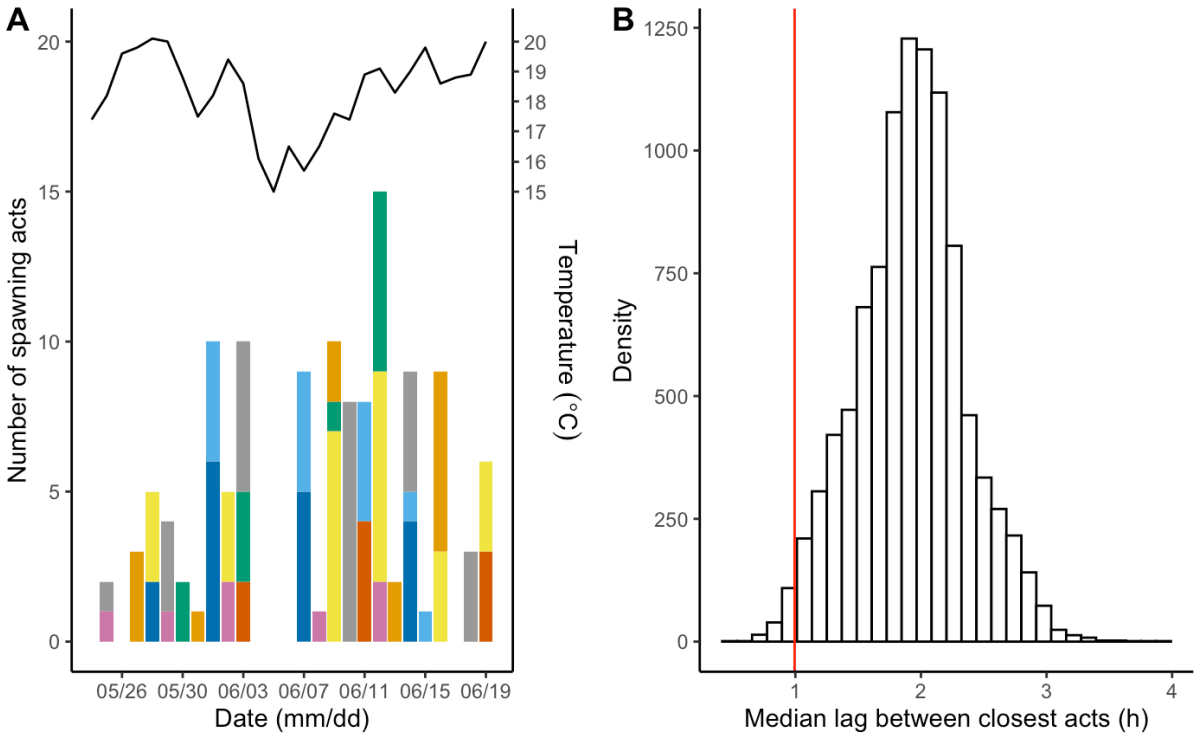

Figure 3. The temporal distribution of spawning acts by eight Allis shad females in the river Nivelle in spring 2017. A. Cumulated number of spawning acts for each night of the season. Each colour corresponds to an individual. The line above the bar plot represents the average water temperature measured each night between 10PM and 7AM. B. Synchrony of spawning acts performed by different females within a night (only the first act of the night, for each female). The red vertical line represents the median time lag between nearest spawning acts for observed data. The histogram represents the same thing for 10 000 permutation of the hour of the acts.

Average tail beat frequency (TBF), temperature and depth were computed for 312 840 minutes across all individuals' spawning seasons (eight complete and one partial). Tail beat frequency ranged from 1.3 to 9.5 beats per second (mean=3.2), temperature ranged from 13.5 to 23.8°C (mean=18.3), and depth ranged from 0 to 400 cm (mean=186).

From equations (1) and (2), the estimated instantaneous rate of energy expenditure ranged from 0.09 to 0.89 $kJ.min^{-1}$ (mean=0.17), and energy expenditure cumulated by each of the eight individuals from initial capture to death ranged from 4 395 to 8 361 kJ (mean=6 277; Fig. 4.A). The corresponding weight loss was estimated to range from 127 to 241 g (mean=181), making from 9% to 17% of initial weight (mean=12%). The shad died 44 to 182 hours (mean=98.62) after their last spawning act. They had lost between 33% and 53% of their weight (mean=42%), and their ovaries weighed 25.9 to 141.5 g (mean=79.7). No correlation was found between weight loss and ovary weight (Spearman S=89.3; rho=-0.06; p=0.888). The predicted and observed weight lost during the season were positively correlated, (Spearman S=8.55; rho=0.9; p=0.002; Fig. 4.B), but the predicted weight loss was on average 1.5 times less than the actual loss (479 g difference on average).

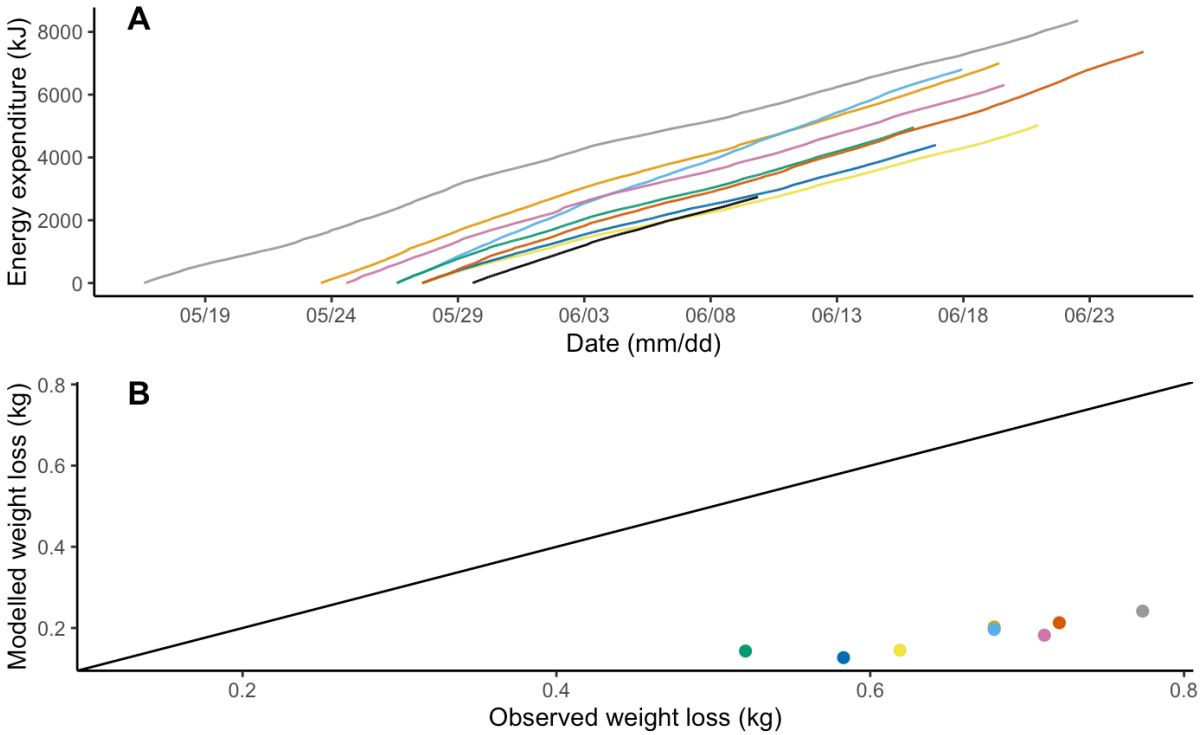

Figure 4. A. Energy expenditure over the spawning season for nine female Allis shad, estimated from temperature and TBF using equations (1) and (2). B. Observed weight loss and weight loss modelled with equations (1) and (2) over the spawning season. The straight line in B is the one on which points should lie if the modelled weight loss would fit the observations. Colours are as in Fig. 3, with black line in A for the individual whose tag stopped recording before the end of the experiment.

Aggregating TBF, temperature and pressure data over 8-hour periods (morning: 6AM-2PM, afternoon: 14PM-10PM, night: 10PM-6AM) produced 649 8-hour periods (Fig. 5). Shad stayed closer to the surface at night than during the morning and afternoon (LRT χ^2=238.9; p<0.0001; R^2_m=0.14; R^2_c=0.69), and underwent warmer temperature in the afternoon than in the night than in the morning (LRT χ^2=15.8; p<0.0001; R^2_m=0.02; R^2_c=0.05). TBF was higher at night than in the afternoon than in the morning (LRT χ^2=26.8; p<0.0001) and was also higher during the first nine periods (three days) just after tagging than afterwards (LRT χ^2=37.6;

443 p<0.0001; R^2_m=0.06; R^2_c=0.36 for the model including both effects). The estimated energy
444 expenditure was the highest at night, followed by afternoon and morning (LRT χ^2=24.8;
445 p<0.0001; R^2_m=0.03; R^2_c=0.34). The mass of eggs remaining at death was not correlated to the
446 energy expenditure cumulated across mornings (Spearman S=66; rho=0.21, p=0.619),
447 afternoons (Spearman S=64; rho=24; p=0.582), nights (Spearman S=76; rho=0.09; p=0.84), or
448 the whole season (Spearman S=64; rho=0.24; p=0.582).
449

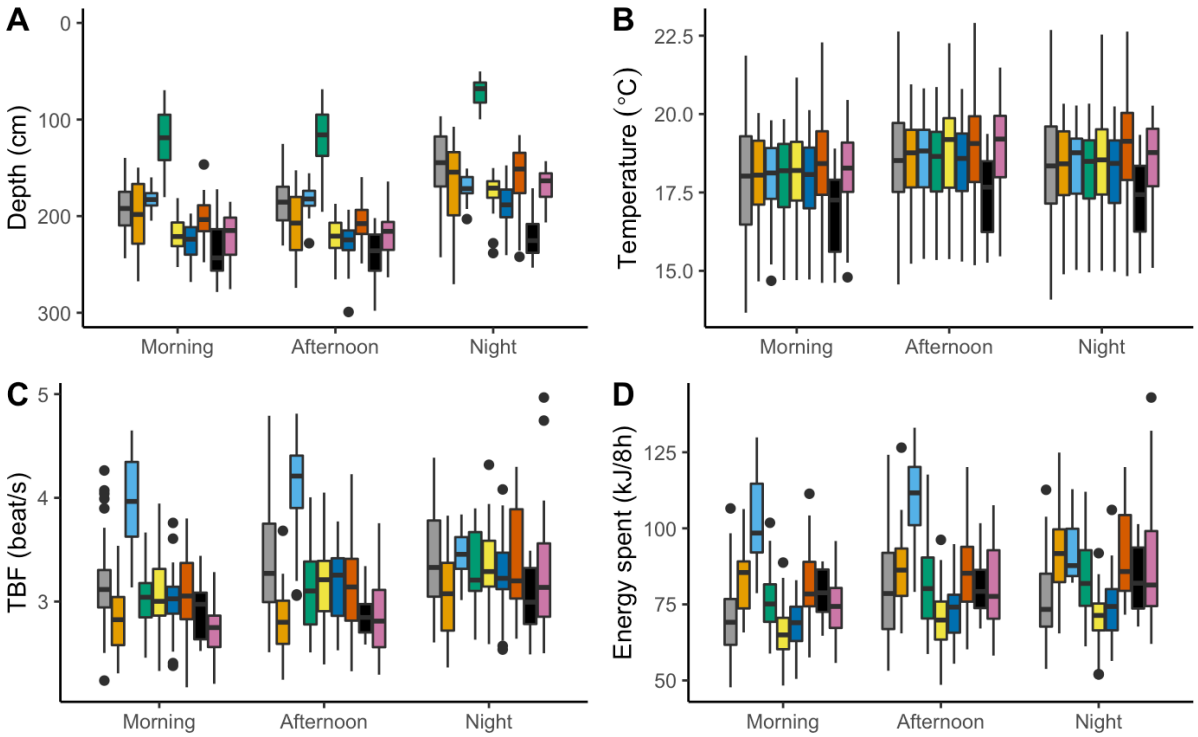

450
451

452 **Figure 5.** Depth (A), temperature (B), tail beat frequency (C) and estimated energy spent (D)
453 by nine female allis shad during the morning (6AM:2PM), afternoon (2PM:10PM) and night
454 (10PM:6AM) of their spawning season. Box plots show the distribution of the variables
455 averaged (A, B, C) or cumulated (D) across 8-hour periods for each individual (colours as in
456 Fig. 3, black for the individual whose tag stopped recording before the end of the experiment).
457 In C, energy spent was computed from temperature and TBF using equations (1) and (2).
458

As expected, the θ angle between the x-axis of the accelerometer and the vertical was positively correlated to the individual's Fulton coefficient of condition (Pearson's r=0.63; p=0.006), although the effect seemed to be due to within-individual difference in condition and θ at the beginning and at the end of the season rather than inter-individual variability in condition and θ (Fig. 6.A). Moreover, the θ angle globally decreased over time for all individuals (LRT χ^2=516.9; p=0.001; R^2_m=0.29; R^2_c=0.78; Fig. 6.B), with a slope of -0.21 degree per eight hours, although it increased during some 8-hours periods. However, contrary to our expectation, the difference of the θ angle between initial capture and death was not related to change in body condition between initial capture and final recapture (Spearman S=76, rho=0.09, p=0.84). The best mixed model to explain the shift in θ during a 8-hour period was the one with the moment (morning, afternoon or night) of the period as the independent factor (LRT χ^2=56.7; p<0.0001; R^2_m=0.08; R^2_c=0.08), followed by the null model including individual random effect only (ΔAICc=51), the model including estimated energy expenditure as the independent variable (ΔAICc=56), and the model including both temperature and TBF as independent variables (ΔAICc=58). According to the best model, the shift in θ was negative during mornings (mean ± standard deviation -1.25° ± 3.08), slightly negative during afternoons (-0.23° ± 2.36), and positive during the nights (0.89° ± 3.15).

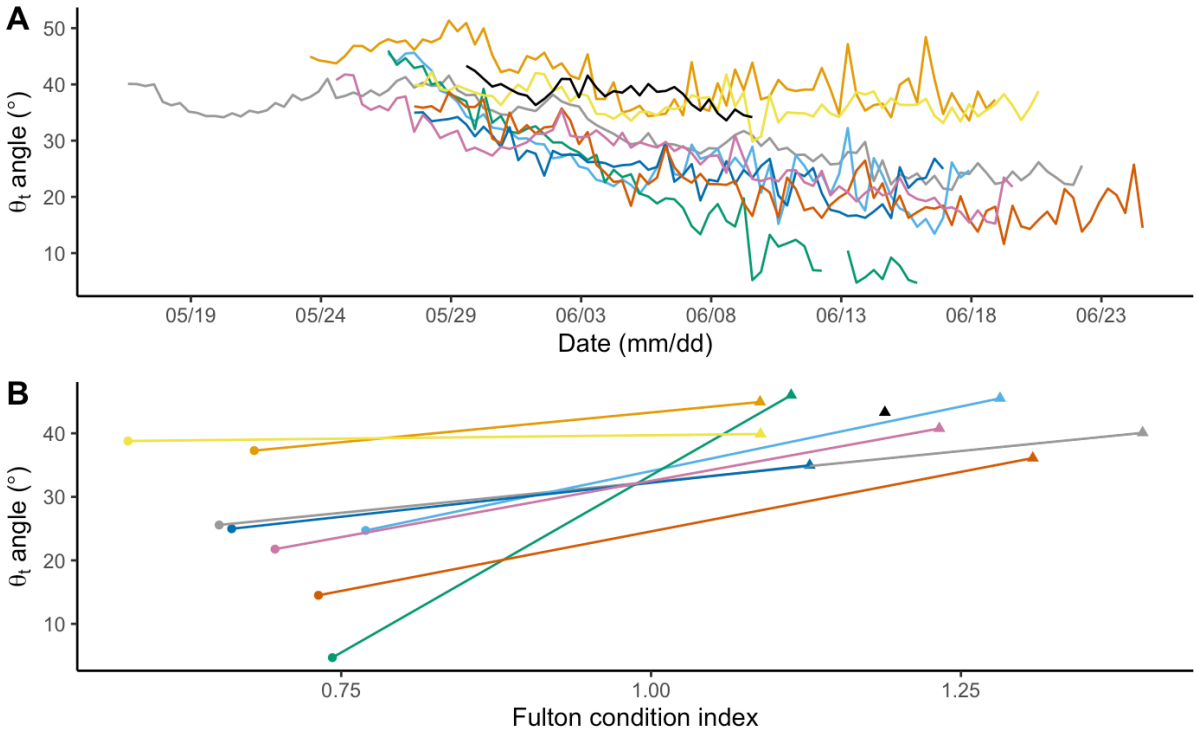

Figure 6. The θ_t angle between the x-axis of the accelerometer and the vertical as an indicator of fish body roundness A. Temporal evolution of θ computed each day along the spawning season for nine Allis shad. B. Relationship between Fulton coefficient of condition and θ_t angle at initial release (triangles) and at recapture after death (points). Each individual is represented with the same colour as in Fig. 3, and black is for the individual whose tag stopped recording before the end of the experiment.

Discussion

In this study, we used acceleration data to quantify the dynamics of spawning acts, energy expenditure and thinning of Allis shad females throughout their spawning season. The results indicate that the spawning schedule of shad females, although constrained by the serial maturation of oocyte batches, was also influenced by temperature and social factors: individual females had a higher probability to spawn during warmer nights, spawned repeatedly during most of their active nights and females that spawned on the same nights synchronized their

spawning acts. Tail beat frequency and water temperature recorded by the loggers showed that energy expenditure was slightly higher during night time than during daytime, and may have been too high to allow shad to spawn all their eggs. Finally, the original use of gravitational acceleration to monitor fish thinning, although perfectible, seems a promising method in animal ecology.

Dynamics of spawning acts and energy expenditure

The number of spawning acts performed by female Allis shad ranged from 7 to 26, with an average of 15.75. So far, the average individual number of spawning acts was indirectly estimated to be either five (Acolas et al., 2006) or 12 (Fatin and Dartiguelongue 1996) by counting the number of acts heard upstream a dam where all passing individuals were censused. Such method provides no estimate of interindividual variability. In a first attempt to work at the individual level, Acolas et al. (2004) marked three females and three males with acoustic tags, and based on the number of detections of the tags near the surface (assessed by the reception power by hydrophones immersed at different depth), estimated that zero, one and two acts were performed by the females and three, 38 and 60 acts by the males. Here, despite a small sample, we estimated a more representative distribution of the number of acts per individual, as their detection on accelerograms is certainly more reliable than the method used by Acolas et al. (2004). This distribution, as well as the timing of spawning acts, is crucial to build a model estimating the number of shad in a river from the acoustic survey of spawning acts, as it is routinely done in European rivers (e.g. Chanseau et al. 2004). Such a model, simulating shad spawning behaviour in an Approximate Bayesian Computation framework (ABC; Csilléry et al. 2010) is available in French here: https://ctentelier.shinyapps.io/alose_abc/. The number of acts per female could be correlated to none of the few biometric variables collected, but the very small sample implied a weak statistical power.

Beside oocyte maturation and temperature, the temporal distribution of spawning acts was aggregated within and among females. While each female was active for most of the population's spawning season, the individual spawning season was punctuated by three to six nights of activity generally corresponding to volleys of two to eight acts performed in a few tens of minutes, and separated by on average 3.5 nights of inactivity. The schedule of spawning acts must be constrained by the fragmented maturation of oocytes (Cassou-Leins and Cassou-Leins 1981; Olney et al. 2001), but also depended on temperature. Interestingly, while data collected at the population level indicate that spawning activity increases with temperature (Paumier et al. 2019), our data collected at the individual level showed that temperature increased the probability that a female performed some acts during the night, but not the number of acts it performed. In fact, two results suggest that the dynamics of spawning acts within a night might be influenced by social factors. First, the temporal proximity of acts performed by a given female in a given night in this study, and the high proportion of acts performed without oocyte expulsion reported by Langkau et al. (2016) remind of female trout's 'false orgasm' (Petersson 2001) or female lamprey's 'sham mating' (Yamazaki and Koizumi 2017). For both of these species, it has been suggested that repeated spawning simulations enable the female to exert mate choice, by both exhausting the sperm stock of an unwanted courtier and signalling its mating activity to peripheral males. Second, spawning acts of different females in a given night were more synchronous than expected from the hour of spawning acts across all nights of the season. This suggests that a female which is ready to spawn (mature batch of oocytes) in a propitious night (warm temperature) may trigger its spawning acts when another female does so. Such fine scale synchrony may again affect sexual selection, reducing the environmental potential for polygyny by making it difficult for the same male to monopolize several females at the same time (Emlen and Oring 1977).

The final point in the spawning schedule of semelparous organisms is death, which struck female shad two to seven days after their last spawning act, and before they laid all their eggs, which suggests that energetic reserves were exhausted before egg stock. Combining acceleration and temperature data collected in the field to equations parametrized in laboratory experiments, we estimated that the energetic expenditure of spawning shad during three weeks of spawning ranged from 4 395 to 8 361 kJ (mean=6 277). This is surprisingly of the same order as female American shad, which entered the Connecticut river with a stock of 12 000 kJ, of which approximately 5 000 kJ were consumed along their 228-km and seven-week long upstream migration in waters warming from 10 to 22°C (Leonard & McCormick, 1999). Extreme pre-spawning energy expenditure caused by long migration, obstacle crossing or warm water can reduce the reproductive lifespan of semelparous females and hinder their ability to spawn their full egg stock (Hruska et al. 2011). While the spawning ground used by shad in our study is only 13 km from the river mouth with only one obstacle to pass (Uxondoa, where we captured them), the median daily temperature recorded in the Nivelle for May and June 2017 was 18.4°C, the second warmest spring since the beginning of record in 1984, the maximum being 18.5°C in 1989, the minimum 14.6°C in 2013, and the median 16.9°C. According to our analysis of data from Leonard et al. (1999; our equation 1), an increase in temperature from 16.9 to 18.4°C would raise the energy expenditure of 8.3%, giving both a possible explanation for the inability of shad to spawn all their eggs before they die and a hint of the impact of global warming on the breeding performance of such species.

As expected from visual observations on spawning grounds, shads were more active at night than during the day, and stayed deeper during daytime when water was warmer. Although nocturnal spawning is usually interpreted as a strategy to decrease predation risk on spawners or eggs (Robertson 1991), resting in deeper, hence fresher, water during the warm hours of the day may also save energy for spawning at night. However, contrary to our predictions, the

565 individuals who spent less energy during mornings or afternoons and more during the night did
566 not have fewer residual eggs at death.
567
568 ## Methodological considerations
569 According to calculated energy expenditure, the energetic model predicted that shad
570 should have lost on average 12% of their initial weight, which was much less than the observed
571 42% loss. Of course, the energetic model did not account for egg expulsion, which must
572 represent a large proportion of weight loss, given that ovaries can represent up to 15% of
573 somatic weight at the onset of the spawning season (Cassou-Leins and Cassou-Leins 1981;
574 Taverny 1991). Moreover, the equations used to convert TBF and temperature to energy
575 expenditure and weight loss were not parametrized with data obtained on *A. alosa* but on *A.*
576 *sapidissima* (Castro-Santos & Letcher, 2010; Leonard et al., 1999; Leonard & McCormick,
577 1999) which is the species most closely related to *A. alosa* for which such reliable information
578 exist. Although American shad and Allis shad have the same morphology and ecology, some
579 elements suggest that results on American shad could not exactly apply to our study on Allis
580 shad. First, although the range of temperatures used by Leonard et al. (1999) were similar to
581 the temperatures encountered by shad in our study, TBF of Allis shad in the field exceeded the
582 fastest swim tested by Leonard et al. (1999). In particular, the brief bouts of very high TBF
583 which correspond to spawning acts may represent anaerobic efforts, which are more costly than
584 the aerobic effort observed by Leonard et al. (1999). The volleys of spawning acts performed
585 by females in a few tens of minutes could even lead to sexual selection of traits affecting the
586 recovery after sprint (Kieffer 2000). Second, the relationship linking swim speed to oxygen
587 demand (MO_2) varies between species, even closely related, and American shad seems to have
588 a particularly high metabolism compared to other clupeids (Leonard et al. 1999). This would
589 have led to an overestimation of energy expense for *A. alosa*. Third, the relative contribution of

lipids and proteins as metabolic fuel may differ between the iteroparous American shad and the semelparous Allis shad. Indeed, as migratory iteroparous fishes have to spare proteins, especially in the red muscle, for their downstream migration, semelparous species can exhaust their protein stock to complete spawning (Schultz 1999). Also, Leonard & McCormick (1999) measured the relative expenditure of lipids and proteins in *migrating* American shad, while we monitored *spawning* Allis shad. It has been shown that most anadromous fishes catabolise proteins only when lipid reserves have been exhausted, in a way that lipids mainly fuel migration while proteins fuel spawning (Idler and Bitners 1958; Beamish et al. 1979; Jonsson et al. 1997; Hendry and Berg 1999). Given that proteins have a lower energy density than lipids, the surprising high energy consumption and the low weight loss predicted by the energetic model may be explained by spawning Allis shad relying more on proteins than on lipids.

While the presence of the radio tag and the accelerometer may have imposed an energetic cost on shad due additional weight (less than 2% of initial fish weight) and drag, several indicators suggest that our tagging method did not impact shad behaviour as heavily than the commonly gastric implants which result in high mortality rate or long post-tagging downstream movements (Steinbach et al. 1986; Verdeyroux et al. 2015; Tétard et al. 2016). Such downstream movements were only observed in 2018, after exceptional floods which have probably also wiped away untagged shad, especially after the spawning season. Although the dead individuals we retrieved in 2017 showed clear depigmentation, neither severe abrasion nor fungal proliferation was observed, even after one month in water at 18° C. Moreover, the eight females for which complete accelerograms were retrieved all spawned, three of them spawned the night directly following tagging, and the median of 14 spawning acts was above the five to twelve acts per individuals estimated by Acolas *et al.* (2006) and Fatin & Dartiguelongue (1996). Tagging did not seem to impair swimming activity either, as tail beat frequency (TBF) was not lower in the three days following tagging than in the remaining of the season. TBF was

615 actually higher during the first three days, probably because the fish were finishing their
616 upstream migration, before settling near spawning grounds (unpublished radio tracking data).
617 This absence of negative impact suggests that external tagging under the dorsal fin, provided
618 fish are continually kept immerged and rapidly handled, is a suitable tagging technique for Allis
619 shad (Jepsen et al. 2015; Breine et al. 2017).

620 On top of the estimation of energetic costs from dynamic acceleration, the continuous
621 estimation of body roundness from static acceleration is a promising yet perfectible application.
622 Gravitational acceleration is commonly used to infer the posture of the animal, assuming that
623 the position of the accelerometer on the animal is constant (Brown et al. 2013). Here, assuming
624 that shad stayed upright for most of the time, gravitational acceleration was used as an indicator
625 of change in body shape. In particular, we hypothesized that the angle θ between the x axis of
626 the accelerometer and the vertical may indicate body roundness. For all individuals, θ was
627 higher at the beginning of the season than at the end, when the fish had thinned, and globally
628 decreased along the spawning season. The accelerometer was attached under the dorsal fin,
629 where the cross-section is the broadest, which probably maximized the sensitivity of
630 acceleration data to fish thinning. Furthermore, shad mainly store energy for migration and
631 spawning as subdermal fat and interstitial fat in the white muscle (Leonard and McCormick
632 1999), whereas the limited consumption of visceral and liver fat may not have affected θ.
633 However, interindividual variability in θ was not correlated to interindividual variability in
634 body condition, and the shift in θ was not correlated to individual weight loss during the
635 spawning season. This could be due to interindividual differences in the exact position of the
636 accelerometers on the fish, or in the relationship between body condition and roundness. Indeed,
637 weight loss due to gamete expulsion was probably undetectable by the accelerometer attached
638 to the back of the fish. Given that ovaries can represent up to 15% of a shad weight at arrival
639 on spawning grounds (Cassou-Leins and Cassou-Leins 1981; Taverny 1991), a significant loss

of weight was probably not reflected in the rotation of the accelerometer across the spawning season. In fact, shift of θ across eight hour periods increased with neither TBF, temperature, nor estimated energy expenditure, contrary to what was expected from the relationship linking TBF and temperature to energy consumption in American shad (Leonard et al. 1999). Additionally, θ increased during some periods (especially nights), and fluctuated a lot especially at the end of the season, so it was clearly affected by other processes than fish thinning. In particular, while the attachment wires were tightened during the tagging procedure, fish thinning loosened them so the accelerometer must have jiggled more and more as fish thinned, thereby increasing the noise in acceleration data. Hence, using the angle of the accelerometer to quantitatively track change in weight or body roundness will certainly require further tuning, such as laboratory experiment with repeated weighing and image analysis of the fish's cross-section, and drastic standardization of attachment procedure, but we consider it a promising method to monitor individual condition in the field. Once refined, this approach could be used to detect the many ecologically or behaviourally relevant changes in animal shape beyond thinning due to energy consumption, such as parturition, massive food intake in large predators (Cuyper et al. 2019), inflammatory swelling (Duncan et al. 2016), or inflation as a courtship or defence behaviour (Wainwright and Turingan 1997). Combined with dynamic acceleration, such data could be used to test whether these changes in shape are associated to global activity or to the expression of specific behaviours.

Acknowledgements

We thank B. Liquet, F. Luthon, B. Larroque and E. Bouix for their help in the initial exploration of data, and J. Leonard and T. Castro-Santos for sharing their data on American shad. This study was financed by the Adour-Garonne Water Agency, and the French region Nouvelle Aquitaine.

664

References

Acolas M, Veron V, Jourdan H, Begout M, Sabatie M, Bagliniere J l. 2006. Upstream migration and reproductive patterns of a population of allis shad in a small river (L'Aulne, Brittany, France). doi:DOI:10.1016/j.icesjms.2005.05.022.

Acolas ML, Anras MLB, Véron V, Jourdan H, Sabatié MR, Baglinière JL. 2004. An assessment of the upstream migration and reproductive behaviour of allis shad (*Alosa alosa* L.) using acoustic tracking. ICES J Mar Sci. 61(8):1291–1304. doi:10.1016/j.icesjms.2004.07.023.

Anderson SS, Fedak MA. 1985. Grey seal males: energetic and behavioural links between size and sexual success. Animal Behaviour. 33(3):829–838. doi:10.1016/S0003-3472(85)80017-8.

Baglinière J-L, Elie P. 2000. Les Aloses (*Alosa alosa* et *Alosa fallax spp*.): écobiologie et variabilité des populations. Editions Quae.

Barton K. 2009. MuMIn: Multimodel inference. https://cran.r-project.org/web/packages/MuMIn/index.html.

Bates D, Maechler M, Bolker B, Walker S. 2014. lme4: Linear mixed-effects models using Eigen and S4.

Beamish FWH, Potter IC, Thomas E. 1979. Proximate composition of the adult anadromous sea lamprey, *Petromyzon marinus*, in relation to feeding, migration and reproduction. Journal of Animal Ecology. 48(1):1–19. doi:10.2307/4096.

Bengen GSH. 1992. Suivi de la maturation gonadique des aloses, Alosa alosa L. lors de leur migration en Garonne. PhD thesis: Institut national polytechnique de Toulouse, France.

Bonnet X, Bradshaw D, Shine R. 1998. Capital versus income breeding: an ectothermic perspective. Oikos. 83(2):333–342.

Borgia G. 1985. Bower quality, number of decorations and mating success of male satin bowerbirds (*Ptilonorhynchus violaceus*): an experimental analysis. Animal Behaviour. 33(1):266–271. doi:10.1016/S0003-3472(85)80140-8.

690 Breine J, Pauwels IS, Verhelst P, Vandamme L, Baeyens R, Reubens J, Coeck J. 2017.
691 Successful external acoustic tagging of twaite shad *Alosa fallax* (Lacépède 1803). Fisheries
692 Research. 191(Supplement C):36–40. doi:10.1016/j.fishres.2017.03.003.
693 Brett JR, Groves TDD. 1979. Physiological energetics. In: Hoar WS, Randall DJ, Brett JR,
694 editors. Bioenergetics and growth. Vol. 8. Academic Press. New York. (Fish physiology). p.
695 279–352.
696 Brooks ME, Kristensen K, Benthem KJ van, Magnusson A, Berg CW, Nielsen A, Skaug HJ,
697 Mächler M, Bolker BM. 2017. glmmTMB balances speed and flexibility among packages for
698 zero-inflated generalized linear mixed modeling. The R Journal. 9(2):378–400.
699 Brown DD, Kays R, Wikelski M, Wilson R, Klimley AP. 2013. Observing the unwatchable
700 through acceleration logging of animal behavior. Animal Biotelemetry. 1(1):1–16.
701 doi:10.1186/2050-3385-1-20.
702 Casas J, Pincebourde S, Mandon N, Vannier F, Poujol R, Giron D. 2005. Lifetime nutrient
703 dynamics reveal simultaneous capital and income breeding in a parasitiod. Ecology. 86(3):545–
704 554. doi:10.1890/04-0812.
705 Cassou-Leins F, Cassou-Leins J-J. 1981. Recherches sur la biologie et l'halieutique des
706 migrateurs de la Garonne et principalement l'alose : *Alosa alosa*. PhD thesis. Institut National
707 Polytechnique de Toulouse.
708 Castro-Santos T, Letcher BH. 2010. Modeling migratory energetics of Connecticut River
709 American shad (*Alosa sapidissima*): implications for the conservation of an iteroparous
710 anadromous fish. Can J Fish Aquat Sci. 67(5):806–830. doi:10.1139/F10-026.
711 Chanseau M, Castelnaud G, Carry L, Martin-Vandembulcke D, Belaud A. 2004. Essai
712 d'évaluation du stock de géniteurs d'alose *Alosa alosa* du bassin versant Gironde-Garonne-
713 Dordogne sur la période 1987-2001 et comparaison de différents indicateurs d'abondance.
714 Bulletin Français de la Pêche et de la Pisciculture.(374):1–19. doi:10.1051/kmae:2004023.

715 Collins PM, Halsey LG, Arnould JPY, Shaw PJA, Dodd S, Green JA. 2016. Energetic
716 consequences of time-activity budgets for a breeding seabird. J Zool. 300(3):153–162.
717 doi:10.1111/jzo.12370.
718 Craig JF, Kenley MJ, Talling JF. 1978. Comparative estimations of the energy content of fish
719 tissue from bomb calorimetry, wet oxidation and proximate analysis. Freshwater Biology.
720 8(6):585–590. doi:10.1111/j.1365-2427.1978.tb01480.x.
721 Csilléry K, Blum MGB, Gaggiotti OE, François O. 2010. Approximate Bayesian Computation
722 (ABC) in practice. Trends in Ecology & Evolution. 25(7):410–418.
723 doi:10.1016/j.tree.2010.04.001.
724 Cuyper AD, Clauss M, Carbone C, Codron D, Cools A, Hesta M, Janssens GPJ. 2019. Predator
725 size and prey size–gut capacity ratios determine kill frequency and carcass production in
726 terrestrial carnivorous mammals. Oikos. 128(1):13–22. doi:10.1111/oik.05488.
727 Duncan AE, Torgerson-White LL, Allard SM, Schneider T. 2016. An evaluation of infrared
728 thermography for detection of bumblefoot (pododermatitis) in penguins. J Zoo Wildl Med.
729 47(2):474–485. doi:10.1638/2015-0199.1.
730 ECP. 2018. Ecology and Fish Population Biology Facility.
731 doi:10.15454/1.5572402068944548E12. http://cnue-pierroton.pierroton.inra.fr:5000/dataset/i-
732 e-ecologie-comportementale-des-poissons.
733 Emlen ST, Oring LW. 1977. Ecology, sexual selection, and the evolution of mating systems.
734 Science. 197(4300):215–223. doi:10.1126/science.327542.
735 Fatin D, Dartiguelongue J. 1996. Etude préliminaire de la reproduction des aloses en 1995 entre
736 Tuilières et Mauzac sur la Dordogne.
737 Føre M, Svendsen E, Økland F, Gräns A, Alfredsen JA, Finstad B, Hedger R, Uglem I. 2020
738 Apr 21. Heart rate and swimming activity as indicators of post-surgical recovery time of
739 Atlantic salmon (*Salmo salar*). doi:10.21203/rs.3.rs-23506/v1.

740 Gauthey Z, Freychet M, Manicki A, Herman A, Lepais O, Panserat S, Elosegi A, Tentelier C,
741 Labonne J. 2015. The concentration of plasma metabolites varies throughout reproduction and
742 affects offspring number in wild brown trout (*Salmo trutta*). Comparative Biochemistry and
743 Physiology Part A: Molecular & Integrative Physiology. 184:90–96.
744 doi:10.1016/j.cbpa.2015.01.025.
745 Groscolas R, Viera V, Guerin N, Handrich Y, Côté SD. 2010. Heart rate as a predictor of energy
746 expenditure in undisturbed fasting and incubating penguins. Journal of Experimental Biology.
747 213(1):153–160. doi:10.1242/jeb.033720.
748 Heimpel GE, Rosenheim JA. 1998. Egg limitation in parasitoids: A review of the evidence and
749 a case study. Biological Control. 11(2):160–168. doi:10.1006/bcon.1997.0587.
750 Hendry AP, Beall E. 2004. Energy use in spawning Atlantic salmon. Ecology of Freshwater
751 Fish. 13(3):185–196. doi:10.1111/j.1600-0633.2004.00045.x.
752 Hendry AP, Berg OK. 1999. Secondary sexual characters, energy use, senescence, and the cost
753 of reproduction in sockeye salmon. Can J Zool. 77(11):1663–1675. doi:10.1139/z99-158.
754 Hicks O, Burthe S, Daunt F, Butler A, Bishop C, Green JA. 2017 Jan 1. Validating
755 accelerometry estimates of energy expenditure across behaviours using heart rate data in a free-
756 living seabird. Journal of Experimental Biology.:jeb.152710. doi:10.1242/jeb.152710.
757 Hruska KA, Hinch SG, Patterson DA, Healey MC. 2011. Egg retention in relation to arrival
758 timing and reproductive longevity in female sockeye salmon (*Oncorhynchus nerka*). Can J Fish
759 Aquat Sci. 68(2):250–259. doi:10.1139/F10-153.
760 Hughes PW. 2017. Between semelparity and iteroparity: Empirical evidence for a continuum
761 of modes of parity. Ecol Evol. 7(20):8232–8261. doi:10.1002/ece3.3341.
762 Idler DR, Bitners I. 1958. Biochemical studies on sockeye salmon during spawning migration:
763 Ii. Cholesterol, fat, protein, and water in the flesh of standard fish. Can J Biochem Physiol.
764 36(8):793–798. doi:10.1139/o58-084.

765 Jepsen N, Thorstad EB, Havn T, Lucas MC. 2015. The use of external electronic tags on fish:
766 an evaluation of tag retention and tagging effects. Animal Biotelemetry. 3(1):49.
767 doi:10.1186/s40317-015-0086-z.
768 Jonsson N, Jonsson B, Hansen LP. 1997. Changes in proximate composition and estimates of
769 energetic costs during upstream migration and spawning in Atlantic salmon *Salmo salar*.
770 Journal of Animal Ecology. 66(3):425–436. doi:10.2307/5987.
771 Kieffer JD. 2000. Limits to exhaustive exercise in fish. Comp Biochem Physiol, Part A Mol
772 Integr Physiol. 126(2):161–179.
773 Kirkendall LR, Stenseth NChr. 1985. On defining 'breeding once'. The American Naturalist.
774 125(2):189–204.
775 Langkau MC, Clavé D, Schmidt MB, Borcherding J. 2016. Spawning behaviour of Allis shad
776 Alosa alosa: new insights based on imaging sonar data. J Fish Biol. 88(6):2263–2274.
777 doi:10.1111/jfb.12978.
778 Leonard JBK, McCormick SD. 1999. Effects of migration distance on whole-body and tissue-
779 specific energy use in American shad (*Alosa sapidissima*). Can J Fish Aquat Sci. 56(7):1159–
780 1171. doi:10.1139/f99-041.
781 Leonard JBK, Norieka JF, Kynard B, McCormick SD. 1999. Metabolic rates in an anadromous
782 clupeid, the American shad (*Alosa sapidissima*). J Comp Physiol B. 169(4–5):287–295.
783 doi:10.1007/s003600050223.
784 Mennesson-Boisneau C, Boisneau P. 1990. Migration, répartition, reproduction,
785 caractéristiques biologiques et taxonomie des aloses (*Alosa sp*) dans le bassin de la loire. PhD
786 thesis. Université de Rennes et Paris XII.
787 Nagy KA, Girard IA, Brown TK. 1999. Energetics of free-ranging mammals, reptiles, and birds.
788 Annu Rev Nutr. 19:247–277. doi:10.1146/annurev.nutr.19.1.247.
789 Olney JE, Denny SC, Hoenig JM. 2001. Criteria for determining maturity stage in female

790 American shad, Alosa sapidissima, and a proposed reproductive cycle. Bull Fr Pêche
791 Piscic.(362–363):881–901. doi:10.1051/kmae:2001025.
792 Paumier A, Drouineau H, Carry L, Nachón DJ, Lambert P. 2019. A field-based definition of
793 the thermal preference during spawning for allis shad populations (*Alosa alosa*). Environmental
794 Biology of Fishes. 102(6):845–855. doi:10.1007/s10641-019-00874-7.
795 Petersson E. 2001. 'False orgasm' in female brown trout: trick or treat? Animal Behaviour.
796 61(2):497–501. doi:10.1006/anbe.2000.1585.
797 Pianka ER. 1976. Natural selection of optimal reproductive tactics. American Zoologist.
798 16(4):775–784.
799 R Development Core Team. 2008. R: A language and environment for statistical computing. R
800 Foundation for Statistical Computing, Vienna, Austria. http://www.R-project.org.
801 Rands SA, Houston AI, Cuthill IC. 2006. Measurement of mass change in breeding birds: A
802 bibliography and discussion of measurement techniques. Ringing & Migration. 23(1):1–5.
803 doi:10.1080/03078698.2006.9674337.
804 Robertson DR. 1991. The Role of adult biology in the timing of spawning of tropical reef fishes.
805 In: Sale PF, editor. The ecology of fishes on coral reefs. San Diego: Academic Press. p. 356–
806 386.
807 Roff D. 1993. Evolution of life histories: Theory and analysis. Springer Science & Business
808 Media.
809 Schultz DL. 1999. Comparison of lipid levels during spawning in annual and perennial darters
810 of the subgenus *Boleosoma*, *Etheostoma perlongum*, and *Etheostoma olmstedi*. Copeia.
811 1999(4):906–916. doi:10.2307/1447966.
812 Stearns SC. 1992. The evolution of life histories. OUP Oxford.
813 Steinbach P, Gueneau P, Autuoro A, Broussard D. 1986. Radio-pistage de grandes aloses
814 adultes en Loire. Bulletin Français de la Pêche et de la Pisciculture.(302):106–117.

815 doi:10.1051/kmae:1986007.

816 Taverny C. 1991. Contribution à la connaissance de la dynamique des populations d'aloses :
817 *Alosa Alosa* et *Alosa Fallax* dans le système fluvio-estuarien de la Gironde : pêche, biologie et
818 écologie : étude particulière de la devalaison et de l'impact des activités humaines. PhD thesis.
819 Bordeaux 1.

820 Tétard S, Feunteun E, Bultel E, Gadais R, Bégout M-L, Trancart T, Lasne E. 2016. Poor oxic
821 conditions in a large estuary reduce connectivity from marine to freshwater habitats of a
822 diadromous fish. Estuarine, Coastal and Shelf Science. 169:216–226.
823 doi:10.1016/j.ecss.2015.12.010.

824 Verdeyroux P, Guerri O, Chanseau M, Cazeaux J, Fauvel F, Bogun F, Desmoulin A, Tarrene
825 C, Nicole T, Dubois A, et al. 2015. Radio-telemetry study of the Allis shad (*Alosa alosa*)
826 migration at Bergerac and Tuilières along the Dordigne river and at Golfech along the Garonne
827 river from 2011 to 2014. Epidor.

828 Wainwright PC, Turingan RG. 1997. Evolution of pufferfish inflation behavior. Evolution.
829 51(2):506–518. doi:10.1111/j.1558-5646.1997.tb02438.x.

830 Wilson RP, White CR, Quintana F, Halsey LG, Liebsch N, Martin GR, Butler PJ. 2006. Moving
831 towards acceleration for estimates of activity-specific metabolic rate in free-living animals: the
832 case of the cormorant. J Anim Ecol. 75(5):1081–1090. doi:10.1111/j.1365-2656.2006.01127.x.

833 Yamazaki C, Koizumi I. 2017. High frequency of mating without egg release in highly
834 promiscuous nonparasitic lamprey *Lethenteron kessleri*. J Ethol. 35(2):237–243.
835 doi:10.1007/s10164-017-0505-0.

836